

# INFLUENCE OF INTRODUCTION OF REFRACTORY PARTICLES INTO WELDING POOL ON STRUCTURE AND PROPERTIES OF WELD METAL

V.V. Holovko, D. Yu. Yermolenko, S.M. Stepanyuk, V.V. Zhukov and V.A. Kostin

E.O. Paton Electric Welding Institute of the NAS of Ukraine

11 Kazymyr Malevych Str., 03150, Kyiv, Ukraine. E-mail: [office@paton.kiev.ua](mailto:office@paton.kiev.ua)

The investigations of influence of change of sizes of primary dfinishrites in the structure of weld metal on their secondary microstructure and mechanical properties were carried out. It is shown that an increase in the width of dfinishrites is accompanied by a rise in the temperature of start of bainite transformation, but the content of low-temperature bainite in the microstructure of weld grows. The possibility of effect of inoculation by dispersed particles of refractory compounds into welding pool on relationship between the content in the microstructure of weld of components with a coarse-acicular and fine-acicular morphology and, accordingly, on mechanical properties of weld was established. 9 Ref., 4 Tables, 10 Figures.

*Keywords:* weld, microstructure, dfinishrites, bainite transformation, inoculation, refractory compounds, mechanical properties

The weld metal can start its crystallization during welding in the form of  $\delta$ -ferrite or austenite of low-alloy steels. From the results presented in [1], it is seen that at the cooling rates of steel melts typical to the weld metal, crystallization begins from the structure of  $\delta$ -ferrite, with which during further cooling solid transformations take place. From the phase diagram of Fe–C it follows that at the temperatures around 1400 °C the formation of austenite begins. The centers of austenite initiation, as a rule, are the boundaries of dfinishrites [2]. The authors of [3] expressed the assumption on the formation of austenite as a result of peritectic reaction between the melt and  $\delta$ -ferrite at the high-energy boundaries of dfinishrites (Figure 1). An important result of this transformation depends on the size of the primary structure, because namely this index is one of the key factors influencing the nature of formation of the secondary structure.

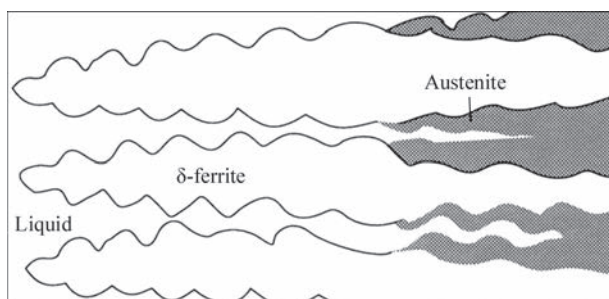


**Figure 1.** Scheme of austenite grain formation on dfinishrites boundaries as a result of peritectic reaction [3]

In the section 1 of [4], it was shown that  $\delta$ -ferrite grains have a columnar morphology and the size of austenitic grains depends on the width of dfinishrites. In order to expand understanding of the peculiarities of forming the secondary structure in the weld metal of low-alloy steels, special investigations were conducted, the results of which are presented in the section 2.

**2. Influence of inoculants on the secondary structure of weld metal.** *2.1. Procedure of experiments.* To study the decay kinetics of supercooled austenite in the metal of the investigated weld, dilatometric tests were performed. During these tests, the metal specimens were subjected to heating and cooling at specified thermal cycles. In the process of thermal effect, dilatometric data were recorded. The specimens of each weld metal were subjected to heating to 1170 °C and cooling. Five thermal cycles were selected, which differed in the cooling rate within the temperature range of 600–500 °C ( $w_{6/5} = 45; 30; 17; 10; 5$  °C/s). The tests were performed in the installation Gleeble 3800.

In the work the procedure of analysis of dilatometric data developed by the authors was applied. To determine critical temperatures of structural-phase transformations, dilatometric data are presented in the form of a diagram of depfinishence of a changed linear size (diameter) of metal specimen during cooling (Figure 2, a). To the linear areas of the obtained dilatogram, which correspond to the law of thermal expansion of ferrite or austenite, the tangents are laid

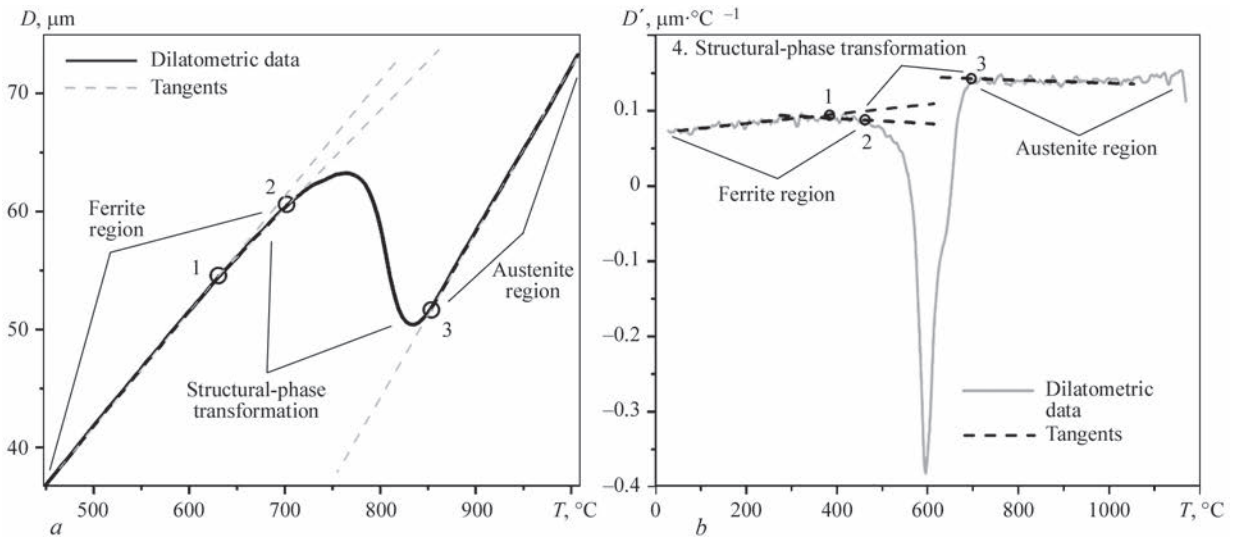


**Figure 2.** Methods for determining critical temperatures of structural-phase transformation by the method of tangents: *a* — on the diagram of depfinescence of dilatometric data on temperature; *b* — on the diagram of depfinescence of the first derivative of dilatometric data on temperature (points 1–3 – critical transformation temperatures, which can be obtained by the method of tangents)

down [5]. The temperature points, at which the tangents begin to deviate from the experimental dilatometric curve, are denoted as the critical temperatures ( $T_n$  and  $T_c$ ) of structural-phase transformations.

However, the accuracy of this method is not high enough [6] and depfines entirely on the choice of temperature range for drawing tangential. The more sensitive method is the method, in which the curves of depfinescence of the first derivative of dilatometric data on temperature are used to draw tangents [7]. It should be noted that, as is seen in Figure 2, *b*, this method is also sensitive to the selection of a linear area on the curve of dilatometric data.

Thermal expansion of solid bodies is not a linear depfinescence on temperature and the formation of a final depfinescence is influenced by many factors [8]. Therefore, to determine the critical temperatures, at which the inverse change of the linear size is observed against the

background of thermal expansion, which is predetermined by the rearrangement of a crystal lattice during structural-phase transformation, we used approximations for the areas corresponding to the temperature depfinescence of linear thermal expansion.

The most accurate results showed empirical depfinescences in the form of polynomials of odd degrees of the following form (Figure 3):

$$F(T) = a_1T + a_2T^3 + a_3T^5 + a_4, \quad (1)$$

where  $F(T)$  is the function of depfinescence of thermal expansion of ferrite or austenite;  $T$  is the temperature;  $a_{1-4}$  are the approximation constants.

Based on the proposed procedure, it was proposed to use the index  $T_V$  to determine the characteristics of transformation.  $T_V$  is the temperature of the maximum intensity of transformation (see Figure 3, *b*). This characteristic has a correlation with the start and fin-

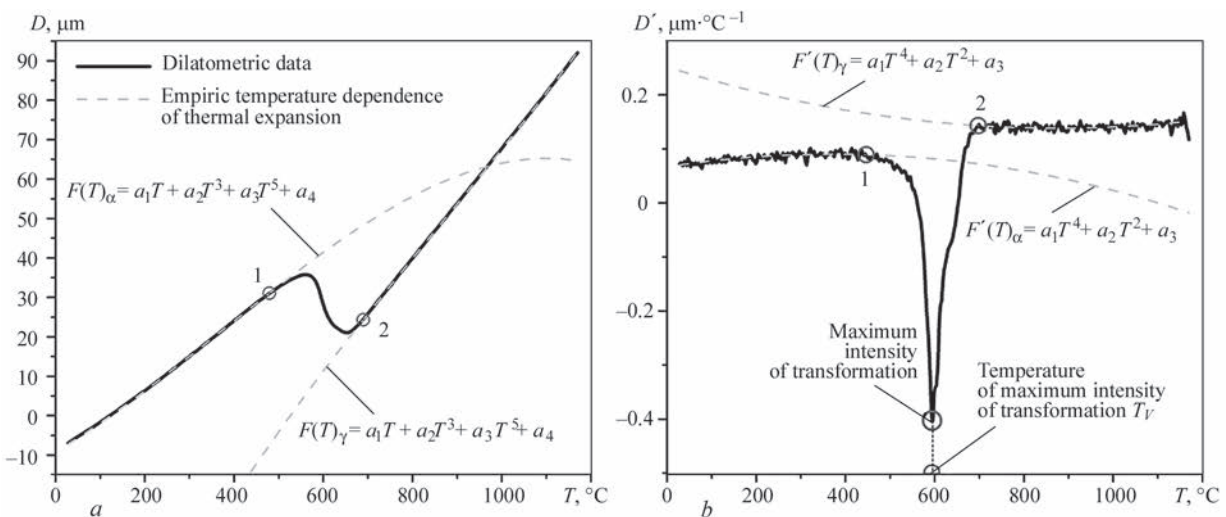


**Figure 3.** Approximation method of analysis of dilatometric data: *a* — approximation of dilatometric data; *b* — approximation of the first derivative (1, 2 — critical transformation temperatures)

**Table 1.** Results of determination of temperatures of phase transformations in weld metal

Weld	$A_{\delta\gamma}$ , °C	$B_s$ , °C	$B_f$ , °C	$\Delta B$ , °C	$\Delta A$ , °C	$T_p$ , °C
BA	870	603.07	443.07	160.00	266.93	567
FeTi	869	583.90	423.10	160.80	285.10	493
TiN	853	589.88	403.04	186.84	263.12	487
VC	863	603.03	412.07	190.96	259.97	549
NbC	893	582.01	431.07	150.94	310.99	534
SiC	851	644.17	435.06	209.11	206.83	540
TiC	870	648.27	435.18	213.09	221.73	562
TiO <sub>2</sub>	885	666.42	431.22	235.2	218.58	559
Al <sub>2</sub> O <sub>3</sub>	890	656.52	437.26	219.26	233.48	559
MgO	873	680.36	457.18	223.18	192.64	574
ZrO <sub>2</sub>	867	687.36	458.07	229.29	179.64	570

*Notes.*  $A_{\delta\gamma}$  is the temperature of start of  $\delta$ - $\gamma$ -transformation;  $B_s$  is the temperature of start of bainite transformation;  $B_f$  is the temperature of finish of bainite transformation;  $\Delta B$  is the temperature range of bainite transformation;  $\Delta A$  is the temperature range of  $\delta$ - $\gamma$ -transformation.

ish temperatures of transformation and can be used as a separate additional index of transformation.

For each weld metal, the values of phase transformation temperatures determined from the diagrams were compared with the results of metallographic analysis of the microstructure. The scheme of sampling for investigations and methods of their etching for metallographic analysis are given in the section 1 [4].

**2.2. Influence on temperature of structural transformations.** To the influence of nonmetallic inclusions on the formation of the microstructure of weld a large number of works is devoted. These works present the results of thermodynamic modeling and data of experimental works on this problem. However, today there is no generalized idea about the mechanisms of influence of dispersed inclusions on the formation of weld metal structure. In connection with the uncertainty of the conditions that determine the content, composition and morphology of nonmetallic inclusions in liquid metal, it is advisable to conduct ex-

periments in which a certain number of chemically pure compounds of a determined size with the known physicochemical indices are artificially introduced into the welding pool. The inoculation of dispersed particles of certain refractory compounds into the welding pool made it possible to investigate the peculiarities of their influence on the size of the structural components of weld metal.

Table 1 shows the results of the analysis of the results of dilatometric investigations, as well as determination of the temperature of the maximum intensity of transformation ( $T_p$ ), performed according to the abovementioned procedures.

**2.3. Secondary structure of weld metal.** Metallographic examinations were performed in a light microscope Neophot-30 with image registration on a computer screen.

The results of metallographic analysis showed that the main structural components of the metal of all investigated joints are upper and lower bainite, differ-

**Table 2** Content of basic structural components in weld metal

Weld	Ferrite					Bainite		Other
	Acicular	Polygonal	Intragranular	Globular	Widmanstatten	Upper	Lower	
BA	10	12	8	16	4	15	26	9
FeTi	6	7	9	17	8	18	30	5
TiC	14	9	9	9	3	19	30	7
TiN	12	10	20	19	16	6	13	4
SiC	5	8	12	16	5	18	33	3
VC	6	9	14	14	14	19	21	3
NbC	7	12	10	6	18	21	15	11
TiO <sub>2</sub>	15	7	15	17	6	17	18	5
Al <sub>2</sub> O <sub>3</sub>	4	19	18	7	15	15	15	7
MgO	18	10	11	10	3	10	33	5
ZrO <sub>2</sub>	20	15	8	6	3	13	30	5



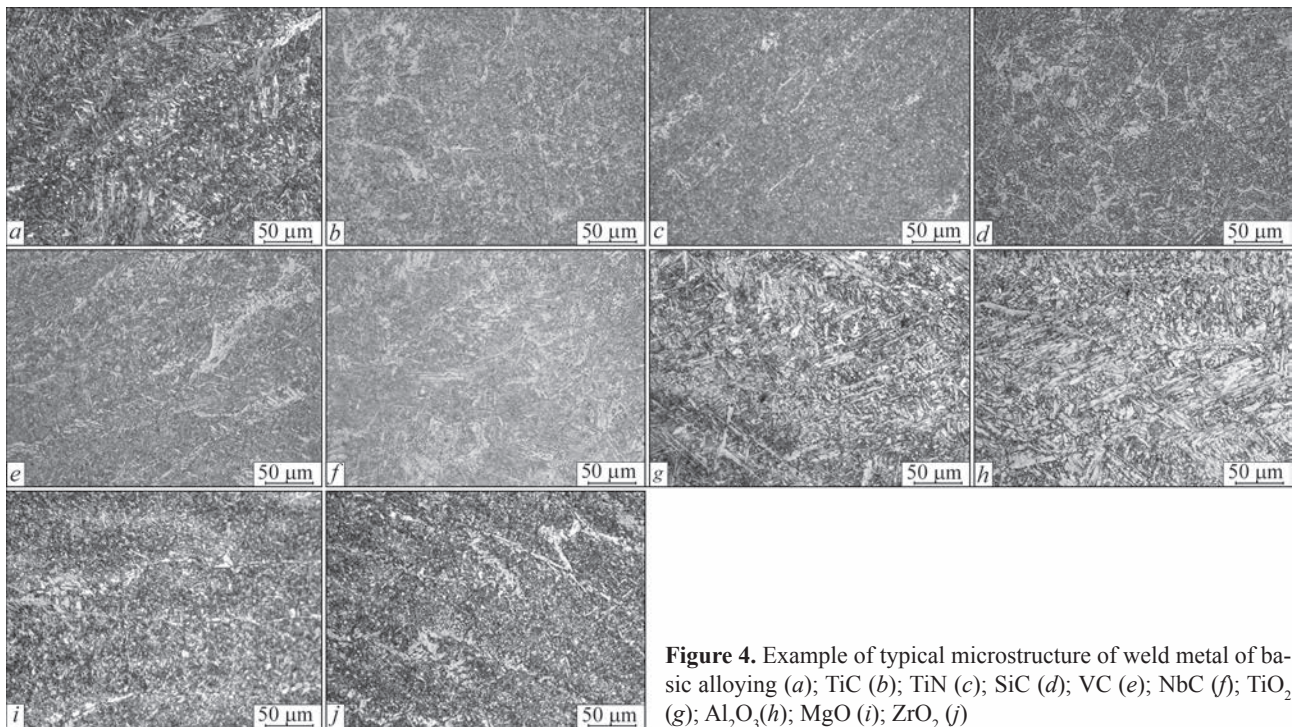


**Figure 4.** Example of typical microstructure of weld metal of basic alloying (a); TiC (b); TiN (c); SiC (d); VC (e); NbC (f); TiO<sub>2</sub> (g); Al<sub>2</sub>O<sub>3</sub>(h); MgO (i); ZrO<sub>2</sub> (j)

ent morphologies of ferrite (acicular, polygonal, intragranular, globular, Widmanstätten) and martensite. The composition of structural components are given in Table 2. Figure 4 shows typical examples of the secondary structure of the weld metal.

Regarding the peculiarities of the structure of particular weld, it should be noted that the weld metal of basic alloying (BA) is characterized by a fine-grained structure with some fragmentation and formation of intravolume dispersed phases.

In the weld metal of FeTi, a nonuniform structure (fine-grained lower bainite and coarse-lamellar upper bainite) is formed at its slight fragmentation with the formation of both intravolume dispersed phases and their clusters along the boundaries.

The structure of TiC weld metal consists mainly of bainitic-ferritic components at a slight fragmentation.

The structure of SiC weld metal contains mainly bainitic-ferritic component at a slight fragmentation with an extfinished spectrum of intravolume dispersed phases and the presence of phase precipitations along the boundaries of a lath structure.

Microstructure of Al<sub>2</sub>O<sub>3</sub> weld metal consists mainly of bainitic-ferritic structure at a slight fragmentation and an extfinished spectrum of intravolume dispersed phases and the presence of phase precipitations along the boundaries of a lath structure.

In the weld metal of ZrO<sub>2</sub> mainly homogeneous bainitic-ferritic structure is formed at the presence of dispersed phase precipitations in the inner volumes of bainitic structure, as well as along the boundaries of fragmented structures.

**2.4. Influence on mechanical properties.** The chemical composition of the weld metal is given in Table 3

**Table 3.** Chemical composition of metal of investigated weld, wt.%

Weld	C	Si	Mn	S	P	Ni	Mo	Al	Ti	Zr	CE <sub>w</sub>
BA	0.034	0.340	1.21	0.021	0.020	2.13	0.28	0.028	0.013	N/D	0.356
FeTi	0.036	0.335	1.22	0.022	0.021	2.14	0.26	0.038	0.029	Same	0.390
TiN	0.035	0.317	1.24	0.019	0.009	2.15	0.26	0.036	0.021	–	0.357
VC	0.052	0.227	1.21	0.022	0.021	2.13	0.25	0.027	0.004	–	0.384
NbC	0.049	0.253	1.19	0.021	0.020	2.15	0.27	0.029	0.003	–	0.387
SiC	0.053	0.351	1.20	0.020	0.025	2.12	0.26	0.025	0.004	–	0.365
TiC	0.046	0.340	1.25	0.021	0.019	2.15	0.24	0.023	0.021	–	0.370
TiO <sub>2</sub>	0.035	0.405	1.24	0.018	0.021	2.17	0.27	0.031	0.027	–	0.332
Al <sub>2</sub> O <sub>3</sub>	0.034	0.424	1.26	0.019	0.023	2.15	0.29	0.042	0.015	–	0.315
MgO	0.031	0.227	1.21	0.025	0.024	2.15	0.29	0.023	0.013	–	0.297
ZrO <sub>2</sub>	0.033	0.223	1.25	0.024	0.024	2.14	0.30	0.024	0.013	0.06	0.303

**Table 4.** Mechanical properties of metal of investigated weld

Weld	$\sigma_y$	$\sigma_{0.2}$	$\delta$	$\psi$	KCV, J/cm <sup>2</sup> at T, °C			
	MPa		%		20	0	-20	-40
BA	685	610	15	54	97	87	75	53
FeTi	747	690	19	60	74	69	63	61
TiC	716	644	19	63	110	97	85	73
TiN	712	580	5.3	14.7	55	47	40	–
SiC	726	650	21	62	85	72	65	61
VC	780	706	14	56	57	55	52	–
NbC	820	757	18	57	45	39	31	–
TiO <sub>2</sub>	709	636	19	57	85	72	60	50
Al <sub>2</sub> O <sub>3</sub>	728	621	17	54	82	58	50	36
MgO	644	586	19	60	103	85	69	60
ZrO <sub>2</sub>	649	592	21	64	97	91	84	76

together with the indices of carbon equivalent, which was calculated according to the standard EN1011-2 [9]. The results of determined mechanical properties of the weld metal are shown in Table 4. From the abovementioned results it is seen that chemical composition of the metal in the investigated weld corresponds to low-alloy steels. The introduction of certain inoculants into the welding pool affected only the content of aluminium and titanium in the weld metal, which can be explained by the peculiarities of deoxidation processes under the influence of introduced joints.

The results given in Table 4, show that introduction of particles of refractory compounds into the welding pool has a noticeable effect on mechanical properties of the weld metal. Such an influence is connected with the changes in the structure of metal, to which this work is devoted.

**2.5. Analysis of investigation results.** In [4], it was shown that introduction of dispersed particles of refractory compounds into the welding pool affects the size of both dfinishrites and grains of a primary austenite. As is seen from Table 2, a significant share of the microstructure components in the investigated weld is represented by morphological forms of bain-

ite. Figure 4 shows the results of comparing the sizes of dendrites formed in the first stages of the welding pool crystallization process [4] with the temperature of start of bainite transformation.

As is seen from the abovementioned data, with an increase in the width of dfinishrites, the temperature of the start of bainite transformation rises. According to the modern notions about the formation of bainite structure, the origination of this phase can be initiated either from the boundaries of austenitic grains or from the middle. If in the first case the initiation of a new phase is controlled by the dislocations density at the grain boundaries, then in the second case it is controlled by the presence of centers of initiation of a new phase in the body of grains of the primary structure. Such centers can be represented by such refractory inclusions as oxides of magnesium, titanium, aluminium, as well as silicon and titanium carbides (Figure 6), which were captured by the crystallization front.

The rate of diffusion of carbon to the interphase boundary in the process of  $\delta$ - $\gamma$ -transformation affects the formation of a lower bainite in the microstructure of the weld metal. As is seen from the abovementioned data, the microstructure of weld, to the compo-

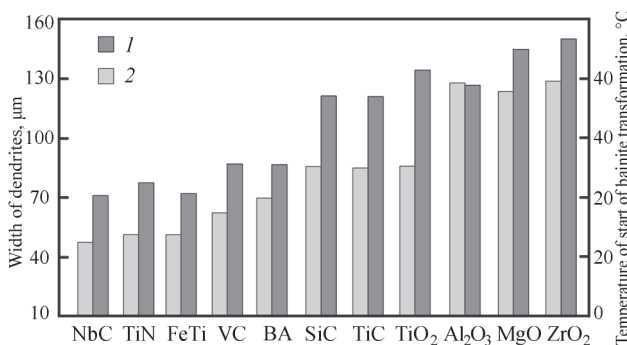


**Figure 5.** Change in temperature of start of bainite transformation (1) depending on width of dfinishrites (2) in the primary structure of weld metal

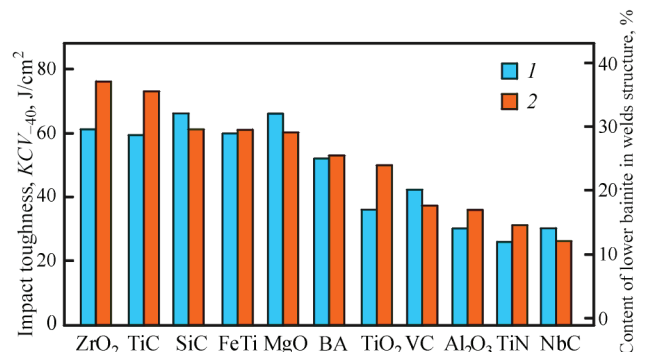


**Figure 6.** Content of lower bainite in the structure (1) and impact toughness (2) of weld metal depending on composition of inoculants

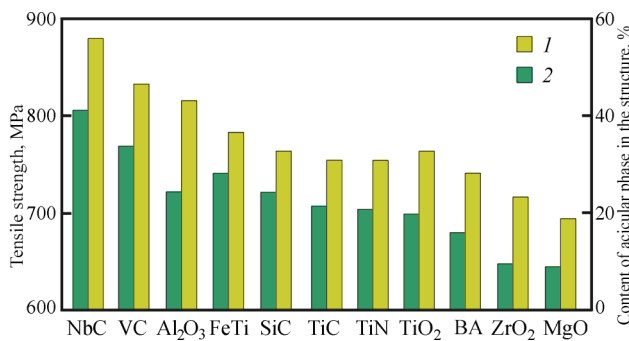


**Figure 7.** Nature of influence of content of coarse-acicular phases between weld metal

sition of which magnesium and zirconium oxides, vanadium and silicon carbides were inoculated, contains an increased amount of a lower bainite. In low-alloy steels, the lower bainite is characterized as a structural component that allows providing the formation of a metal with a high level of toughness while maintaining the appropriate strength.

Two forms of bainite in the metal of low-alloy steels differ both in the nature of a carbide phase formation as well as in their morphology. If during the formation of the upper bainite a significant part of carbon diffuses at the boundary of ferritic grains, where it is precipitated in the form of cementite, then the lower bainite is characterized by precipitation of small carbides in the body of ferritic grains. The lower bainite is formed in the form of a fine-grained structure with small-angle grain boundaries. Such a structure has an increased resistance to the propagation of brittle cracks. The structure of the upper bainite consists of coarser needles with an increased grain disorientation. An increase of the upper bainite together with the second coarse-acicular structural component — Widmanstätten ferrite in the weld of the structure — helps to increase the strength of the metal, but reduces its toughness. The nature of the influence of the total content in the structure of the upper bainite and Widmanstätten ferrite on the yield strength of the weld metal is shown in Figure 7.

The results obtained after the carried out experiments showed that the change in the morphology of dfinishrites at the initial stages of crystallization during inoculation to the welding pool of dispersed particles of refractory compounds, which was reported in [4], affects the peculiarities of formation of secondary microstructure and complex mechanical properties of weld metal.

Based on the application of the proposed parameter of  $T_V$  transformation, the effect of alloying was established (carbon equivalent  $CE_w$ ) on the transformation temperature  $T_V$ ) (Figure 8).

It was found that with a decrease in a carbon equivalent  $CE_w$ , the transformation temperature  $T_V$

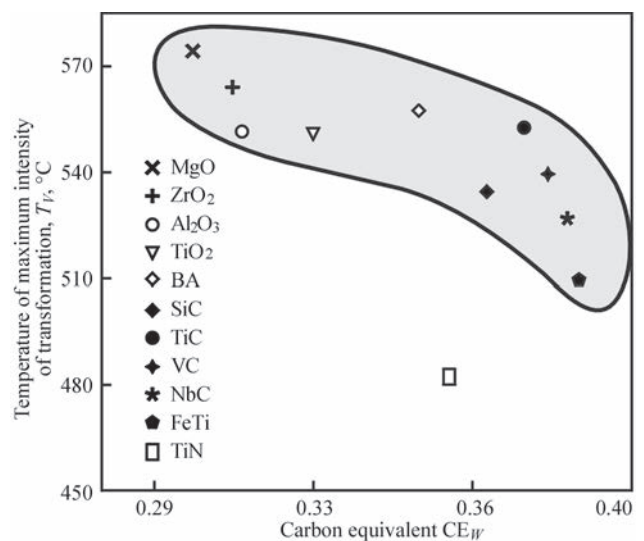


**Figure 8.** Influence of chemical composition of weld metal  $CE_w$  on transformation temperature  $T_V$

increases nonlinearly. It is shown that inoculation of oxides MgO, ZrO<sub>2</sub>, TiO<sub>2</sub> into the weld metal increases the temperature  $T_V$ , while the introduction of carbides TiC, SiC and NbC, on the contrary, reduces it. The difference in the transformation temperatures ranges from 20 to 50 °C.

It is shown that the index of temperature  $T_V$  can be used to analyze the ratio of structural components in the metal of the weld of high-strength low-alloyed steels, as is shown in Figure 9.

It was found that a decrease in the temperature  $T_V$  increases the share of bainitic acicular structures. To the greatest extent, an increase in the share of acicular bainitic structures is influenced by SiC and NbC carbides, which is accompanied by a corresponding increase in strength of weld metal (Table 4, Figure 6) and decrease in the level of impact toughness of weld metal (Table 4, Figures 7 and 10)

The analysis of the obtained results showed that the modification of the weld metal with oxide parti-

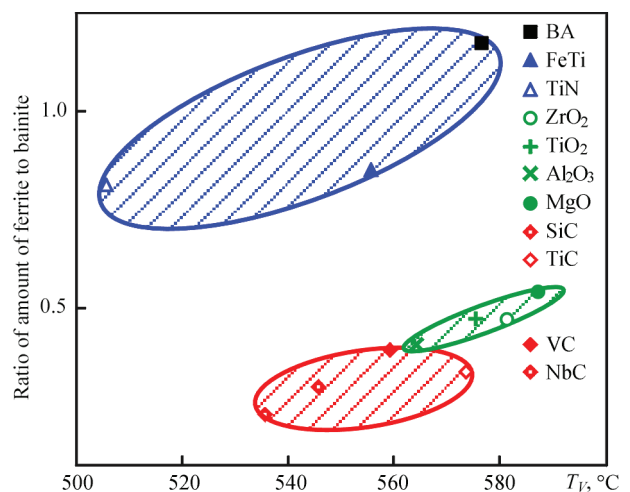


**Figure 9.** Influence of transformation temperature  $T_V$  on ratio of structural (F/B) components



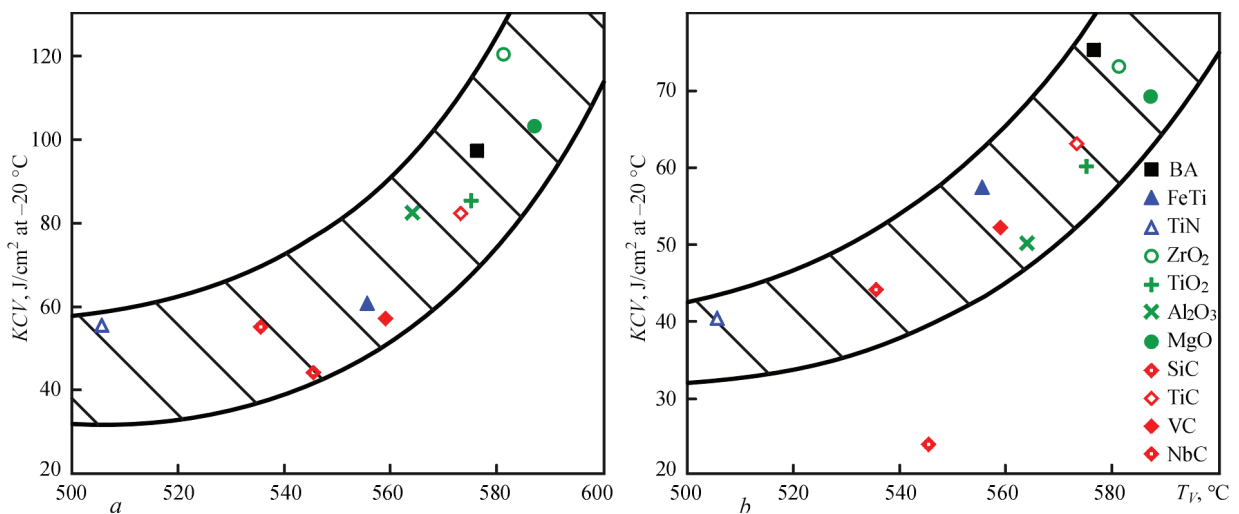


**Figure 10.** Influence of transformation temperature  $T_V$  on toughness of weld metal at different test temperatures:  $a$  — 20;  $b$  — -20 °C

cles ( $ZrO_2$ ,  $TiO_2$ ) is optimal from the point of view of forming the fine-acicular structure of the lower bainite, which provides a high complex of mechanical properties — a combination of high strength, ductility and toughness at low climatic test temperatures.

### Conclusions

The influence of change in the size of  $\delta$ -finishrites, which occurs during inoculation of dispersed particles of refractory compounds into the welding pool, on the formation of the secondary microstructure and mechanical properties of weld metal of low-alloy steels was investigated, as a result of which it was established that:

1. An increase in the width of  $\delta$ -finishrites is accompanied by a rise in the temperature of start of the bainite transformation.

2. Despite an increase in the temperature of start of bainite transformation in the weld metal with an increased width of  $\delta$ -finishrites in the process of cooling, the microstructure with a high content of the lower bainite is formed. This may indicate the inhibition of the diffusion of carbon from austenitic grains during the  $\delta$ - $\gamma$ -transformation in the weld metal inoculated with oxides of magnesium and zirconium, as well as silicon and titanium carbides.

3. A decrease in the width of  $\delta$ -finishrites as compared to the variant of basic alloying is accompanied by a rise in the content of structural components of a coarse-acicular morphology in the metal of weld.

4. Depfinishing on the ratio of the components of a fine-acicular and a coarse-acicular morphology in the microstructure of the weld, the level of strength and toughness of the metal changes.

5. The use of the index of transformation temperature  $T_V$  to describe the influence of thermokinetic pa-

rameters on the formation of metal structure of weld was proposed.

6. Inoculation of dispersed particles of refractory compounds into the welding pool affects the change in the size of  $\delta$ -finishrites of the primary structure and, accordingly, the formation of the secondary microstructure of the weld metal and their mechanical properties.

1. Hideyuki, Y., Takahiro, H., Naoki, S. et al. (2019) Investigation using 4D-CT of massive-like transformation from the  $\delta$  to  $\gamma$  phase during and after  $\delta$ -solidification in carbon steels. *IOP Conf. Series: Mater. Sci. & Engin.* doi:10.1088/1757-899X/529/1/012013, 1–8.
2. Phelan, D., Dippenaar, R. (2004) Instability of the delta-ferrite/austenite interface in low carbon steels: The influence of delta-ferrite recovery sub-structures. *ISIJ Int.*, 44(2), 414–421.
3. Svensson, L.-E. (2000) *Control of microstructures and properties in steel arc weld*. CRC Press, Inc. Corporate Blvd.
4. Holovko, V.V., Yermolenko, D.Yu., Stepanyuk, S.M. (2020) The influence of introducing refractory compounds into the weld pool on the weld metal  $\delta$ -finishritic structure. *The Paton Welding J.*, 6, 2–8.
5. Selivanova, O.V., Polukhina, O.N., Khotinov, V.A., Farber, V.M. (2017) *Modern methods of investigation of polymorphous transformations in steels*: Manual. Ekaterinburg, Ural'sky Un-t [in Russian].
6. Teplukhina, I.V., Golod, V.M., Tsvetkov, A.S. (2018) Plotting of overcooled austenite decomposition diagrams in steel on the base of numerical analysis of dilatometric testing results. *Pisma o Materialakh*, 8(1), 37–41 [in Russian].
7. Motycka, P., Kover, M. (2012) Evaluation methods of dilatometer curves of phase transformations. In: *Proc. of 2<sup>nd</sup> Int. Conf. on Recent Trfinishes in Structural Materials, COMAT 2012 (21–22.11.2012, Plzen, Czech Republic)*, EU.
8. Novikova, S.I. (1976) *Heat expansion of solids*. Moscow, Nauka [in Russian].
9. *EN 1011-2: Welding — Recommenfinishations for welding of metallic materials. Pt 2: Arc welding of ferritic steels*. British Standards Institution, March 2001 AMD A1 Dec. 2003.

Received 30.04.2020